Coordination with binary controllers

Jafarian, Matin

Chapter 7

Formation control of a multi-agent system subject to Coulomb friction

This chapter presents formation control of a network of planar heterogeneous dynamic point masses subject to Coulomb friction in the port-Hamiltonian framework. For dynamic agents, the dissipation due to friction forces plays an important role in stability analysis of the whole network. In the current literature, only continuous friction forces are considered for the formation control problem. This chapter considers formation control of a group of agents in the presence of Coulomb friction which is a discontinuous friction law [24, 84]. Coulomb friction is a quantification of the friction force that exists between two (dry) surfaces in contact with each other. Coulomb friction renders the networked system nonsmooth, thereby requiring tools from nonsmooth systems for the analysis.

This chapter considers a network of point masses moving in $\mathbb{R}^2$ and assume that each of the agents is subject to Coulomb friction. To achieve the desired formation, we consider assigning two types of virtual springs between the agents: continuous and discontinuous (binary) springs. This discontinuity prevents continuous springs to achieve the formation control objectives which is the motivation behind proposing discontinuous springs for the control. Both the network and the controller are modeled within the port-Hamiltonian framework which provides a clear physical interpretation of the results. The results of this chapter are based on [48, 50], in collaboration with E. Vos and A.J. van der Schaft.

The outline of this chapter is as follows. Section 7.1 presents a port-Hamiltonian model for the agents which are subject to Coulomb friction in $\mathbb{R}$ and $\mathbb{R}^2$. Section 7.2 continues with the control design and the closed-loop analysis for both continuous and discontinuous springs. Section 7.3 illustrates the effectiveness of the approach by simulation results. Finally, Section 7.4 concludes the chapter.

7.1 Problem formulation

The goal of this chapter is to design a distributed control law for a network of agents in order to achieve a desired formation at zero momentum (velocity). The communication topology is assumed to be a tree graph (see Chapter 2, Definition 2.1). Let $z_\ell \in \mathbb{R}^2$ denote the relative position between two agents which are interconnected by virtual spring ℓ and let $z_\ell^* \in \mathbb{R}^2$ denote the desired relative position. The formation control objective is to make the relative position $z = (z_1, \ldots, z_m)$ converge to a desired prescribed relative position

$z^* = (z_1^*, \ldots, z_m^*)$ (i.e., achieve a formation). Furthermore, let $p = (p_1, \ldots, p_n) \in \mathbb{R}^{2n}$ denote the momentum vector of the agents (see the agent dynamics (7.4)). We formulate the control objective as follows

$$\begin{cases} p \to \mathbf{0}, \\ z \to z^*, \end{cases} \quad \text{as } t \to \infty. \tag{7.1}$$

To achieve (7.1), we present and compare two types of controllers (virtual springs): a continuous and a discontinuous controller. We show that only the discontinuous controller achieves (7.1) exactly. In the remainder of this section we continue with deriving the dynamical model of the agents. But first, we present a motivational example (in $\mathbb{R}$) to provide some intuition on the differences between continuous and discontinuous virtual springs.

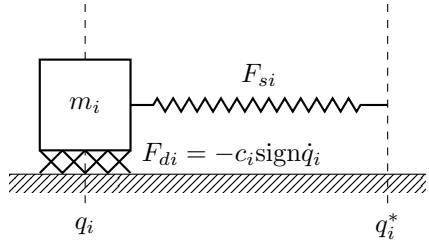

Figure 7.1: System of the motivational example: mass m_i is subject to a Coulomb friction force F_{di} and is controlled by a virtual spring force F_{si}.

Example 7.1 (motivation) *Consider a single mass m_i moving in $\mathbb{R}$ with position $q_i \in \mathbb{R}$ (see Fig. 7.1). The mass is subject to a Coulomb friction force $F_{di} = -c_i \operatorname{sign} \dot{q}_i$ [85], with friction coefficient c_i and velocity $\dot{q}_i \in \mathbb{R}$. Assume that the control objective is to move m_i to a prescribed position q_i^*. We achieve this by assigning a virtual spring to m_i with corresponding spring force F_{si}. We consider two types of springs: a continuous spring where $F_{si}(q_i) = k_i\, q_i$ and a discontinuous spring where $F_{si}(q_i) = k_i \operatorname{sign} q_i$.*
In order to get m_i moving, the virtual spring needs to overcome a friction threshold *of $\pm c_i$. Intuitively, as long as $q_i - q_i^* > \frac{c_i}{k_i}$ the continuous spring gets m_i moving, but once $q_i - q_i^* \leq \frac{c_i}{k_i}$ mass m_i comes to a hold. Hence the control objective might not be achieved. On the other hand, the discontinuous spring provides a spring force of $\pm k_i$ as long as $q_i - q_i^* \neq 0$. Hence, if $k_i > c_i$ the control objective is achieved.*

The example above provides some intuition why the continuous virtual springs might not achieve (7.1), while the discontinuous counterpart achieves the desired goals. Before presenting the two controller designs, we first derive the agents' dynamics.

7.1.1 Dynamical model of agents subject to Coulomb friction

Consider a point mass m_i and let q_i denote its position. Assume that the mass is subject to the Coulomb friction force $F_i(v_i)$, with $v_i = \dot{q}_i$ the velocity of the mass. The Coulomb

friction force for mass m_i moving in $\mathbb{R}$ [48,84,85] is given by

$$F_i(v_i) := \begin{cases} \{c_i \text{sign} v_i\} & \text{if } v_i \neq 0 \\ [-c_i, c_i] & \text{if } v_i = 0 \end{cases}, \tag{7.2}$$

where the function $\text{sign} : \mathbb{R} \to \{-1, +1\}$ is defined as $\text{sign} v_i = +1$ if $v_i \geq 0$ and $\text{sign} v_i = -1$ if $v_i < 0$. Now consider mass m_i moving in $\mathbb{R}^2$. The model of Coulomb friction in $\mathbb{R}^2$ is a bit more involved. Instead of having two decoupled friction forces along the x and y direction, here we consider a more natural model for the friction force that is defined along the direction of motion. We present the model for the Coulomb friction force acting on mass m_i as a set-valued map $F_i : \mathbb{R}^2 \mapsto \mathbb{R}^2$, where $F_i(v_i)$ is given by

$$F_i(v_i) := \begin{cases} c_i \frac{v_i}{\|v_i\|} & \text{if } v_i \neq \mathbf{0} \\ B(\mathbf{0}, c_i) & \text{if } v_i = \mathbf{0} \end{cases}, \tag{7.3}$$

with $c_i \in \mathbb{R}^+$ the friction coefficient and $B(\mathbf{0}, c_i)$ a disc with radius c_i centered at the origin (see Fig. 7.2). Both (7.2) and (7.3) are set-valued maps and their definitions are in accordance with the definition of the Krasovskii map for $\text{sign} v$ in $\mathbb{R}$ and $\mathbb{R}^2$ respectively (see Preliminaries on nonsmooth analysis).

Remark 7.1 *The disc $B(\mathbf{0}, c_i)$ has a clear physical interpretation. When agent i stands still, the controller needs to overcome a threshold of $\pm c_i$ before the agent starts moving. The disc $B(\mathbf{0}, c_i)$ represents the physical fact that there is a friction force even though the agent might not be moving. This corresponds to the situation where the magnitude of the control input is too small to overcome the threshold value.*

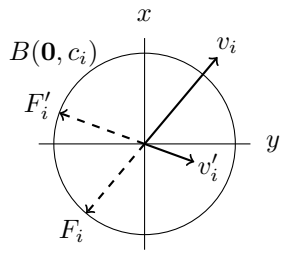

Figure 7.2: Illustration of the Coulomb friction force in $\mathbb{R}^2$ (7.3).

Now consider agent i with position $q_i = (q_{xi}, q_{yi})$ and momentum $p_i = (p_{xi}, p_{yi}) = M_i \dot{q}_i$, with mass $M_i = m_i I_2$. Let $u_i = (u_{xi}, u_{yi})$, $y_i = (y_{xi}, y_{yi})$ and $u_i^r = (u_{xi}^r, u_{yi}^r)$, $y_i^r = (y_{xi}^r, y_{yi}^r)$ denote the port-variables of the control port and the resistive port respectively (see Chapter 2). Here, the inputs u_i, u_i^r are forces, while the corresponding outputs y_i, y_i^r are the velocities of agent i. The dynamics of agent i may now be written in the form (2.6)

as [48]

$$\begin{aligned} \dot{q}_i &= \frac{\partial H_i^a}{\partial p_i}, \\ \dot{p}_i &= -\frac{\partial H_i^a}{\partial q_i} + u_i + u_i^r, \\ y_i = y_i^r &= \frac{\partial H_i^a}{\partial p_i}, \end{aligned} \tag{7.4}$$

where the Hamiltonian $H_i^a(p_i) = \frac{1}{2m_i} p_i^2$ equals the kinetic energy of agent i. The resistive port relation is set as $u_i^r = -F_i(y_i^r)$. From (7.3) it immediately follows that

$$\begin{cases} {y_i^r}^T u_i^r = -c_i \frac{\|y_i^r\|^2}{\|y_i^r\|} < 0 & \text{for } y_i^r \neq 0 \\ {y_i^r}^T u_i^r = 0 & \text{for } y_i^r = 0. \end{cases} \tag{7.5}$$

The above implies ${y_i^r}^T u_i^r \leq 0$ (i.e., the resistive element dissipates power) which means that each agent i is output passive with respect to its velocity.

Now consider a network of n agents of the form (7.4). To derive the dynamics of the network in a compact form, define the stacked vectors $q = (q_1, \ldots, q_n)$, $p = (p_1, \ldots, p_n)$, $u = (u_1, \ldots, u_n)$, $u^r = (u_1^r, \ldots, u_n^r)$, $y = (y_1, \ldots, y_n)$, $y^r = (y_1^r, \ldots, y_n^r)$, and mass matrix $M = \text{block.diag}\,(M_1, \ldots, M_n)$. The dynamics of the network follows directly from (7.4) and is given by

$$\begin{aligned} \dot{q} &= \frac{\partial H^a}{\partial p}, \\ \dot{p} &= -\frac{\partial H^a}{\partial q} + u + u^r, \\ y = y^r &= \frac{\partial H^a}{\partial p}, \end{aligned} \tag{7.6}$$

with Hamiltonian $H^a(p) = \sum_{i=1}^n H_i^a(p_i) = \frac{1}{2} p^T M^{-1} p$ and $u^r = -F(y^r)$ where $u_i^r = -F_i(y_i^r)$ (see (7.3)).

7.2 Control design and analysis

In this section we present two types of controllers for agents of the form (7.6) to achieve the formation control objectives (7.1). Each of the controllers acts like a virtual spring which is assigned in between the agents. The prescribed relative position z_ℓ^* for $\ell \in \{1, \ldots, m\}$ corresponds to the desired relative position amongst the two agents which are interconnected by spring ℓ. We make a distinction between continuous and discontinuous (binary) virtual springs [48] in order to achieve the position-based formation control in terms of [1, 4].

Before continuing with the analysis of the two types of springs, we present the formal analysis of the motivational example in Section 7.1.

7.2.1 Formal analysis of the motivational example

Recall the motivational example in Section 7.1, where mass m_i is subject to a Coulomb friction force F_{di} and is controlled by a virtual spring force F_{si} (see Fig. 7.1). For simplicity we assume that the control objective is to reach a zero distance from the wall (i.e., $q_i^* = 0$). The port-Hamiltonian dynamics are obtained from (7.4) by taking $H^a = \frac{1}{2m}p^2$. We obtain

$$\begin{aligned} \dot{q} &= \frac{p}{m}, \\ \dot{p} &= u + u^r, \\ y = y^r &= \frac{p}{m}, \end{aligned} \tag{7.7}$$

where u is the control law (the spring force) and u^r is the Coulomb friction force defined in (7.2). Hence, $u^r = F(\frac{p}{m})$ is

$$F(\frac{p}{m}) = \begin{cases} c\{\operatorname{sign}\frac{p}{m}\} & \text{if } \frac{p}{m} \neq 0, \\ [-c, c] & \text{if } \frac{p}{m} = 0. \end{cases}$$

Considering the above set-valued map, the dynamics (7.7) can be rewritten as

$$\begin{aligned} \dot{q} &= \frac{p}{m}, \\ \dot{p} &\in -F\left(\frac{p}{m}\right) + u, \\ y = y^r &= \frac{p}{m}. \end{aligned} \tag{7.8}$$

As mentioned in the Preliminaries, we adopt a Krasovskii notion of solution to analyze the solutions of the above differential inclusion.
Now, we consider two types of controllers. First, consider a continuous virtual spring of the form

$$u = -\frac{\partial H^c}{\partial q} = -kq,$$

with corresponding potential spring energy $H^c = \frac{1}{2}kq^2$. The closed-loop Hamiltonian is $H(p, q) = H^a(p) + H^c(q)$. To analyze the stability and convergence of the solutions of (7.8), take $H(p, q)$ as the candidate Lyapunov function and calculate its set-valued derivative (for brevity we skip the calculation of set-valued derivative here). We obtain $\dot{\dot{H}} \in -\frac{p}{m}F(\frac{p}{m}) \subseteq (-\infty, 0]$. Now, applying the nonsmooth LaSalle's invariance principle [13], the system converges to the largest weakly invariant set where $0 \in \dot{\dot{H}}$. The latter implies that on the invariant set $p = 0$. Substituting $p = 0$ in (7.8), we conclude that $\dot{q} = 0$ and therefore $q = q^{eq}$ where q^{eq} is a constant. Moreover, we obtain

$$0 \in [-c, c] - kq^{eq}$$

which implies $q^{eq} \in [-\frac{c}{k}, \frac{c}{k}]$. In other words, the position q converges to a value in an interval containing the origin. Therefore, convergence of the position to zero cannot be guaranteed.

Second, consider a discontinuous (binary) spring where the potential spring energy is $H^d = k|q|$. The control law u is equal to the Clarke generalized gradient [3] of H^d, that is

$$u = \begin{cases} -k\{\text{sign}q\} & \text{if } q \neq 0 \\ [-k, k] & \text{if } q = 0. \end{cases}$$

The closed-loop Hamiltonian is now $H(p,q) = H^a(p) + H^d(q)$, which is locally Lipschitz and regular [3]. Same as the previous case, we take $H(p,q)$ as the candidate Lyapunov function and obtain $\dot{\tilde{H}} \in -\frac{p}{m}F(\frac{p}{m}) \subseteq (-\infty, 0]$. Now, applying the nonsmooth LaSalle's invariance principle, the system converges to the largest weakly invariant set where $p = 0$. Substituting $p = 0$ in (7.8), we conclude that $\dot{q} = 0$ and therefore $q = q^{eq}$ where q^{eq} is a constant. If $q^{eq} > 0$, we have

$$0 \in [-c, c] - k.$$

If $q^{eq} < 0$, we obtain

$$0 \in [-c, c] + k.$$

Now, assume that $k > c$. Therefore, for $q^{eq} > 0$ both the lower and upper bounds of the interval $[-(c+k), c-k]$ are negative, while for $q^{eq} < 0$ both of the bounds of $[-c+k, c+k]$ are positive. Since zero cannot belong to these intervals, we conclude (by contradiction) that q^{eq} is necessarily equal to zero for $k > c$.

The above example provides the motivation for the design and analysis of continuous and discontinuous virtual springs for formation control in the presence of Coulomb friction. We now continue with the dynamics, interconnection structure, control design and closed-loop analysis for a network of point masses in $\mathbb{R}^2$ controlled by continuous and discontinuous virtual springs.

7.2.2 Continuous virtual springs

In this chapter, we pursue the position-based formation keeping control which aims at a desired shape and a desired orientation for the network of agents [4]. For both types of virtual springs, we assign one spring along the x direction and one spring along the y direction. Let spring ℓ represents the relative position, z_ℓ, between two agents. For spring ℓ consider the relative position $z_\ell = (z_{x\ell}, z_{y\ell})$, desired relative position $z^*_\ell = (z^*_{x\ell}, z^*_{y\ell})$, spring constants $K_\ell = \text{diag}\, k_{x\ell}, k_{y\ell}$, and let $\tilde{z}_\ell = (\tilde{z}_{x\ell}, \tilde{z}_{y\ell})$ denote the error variable defined as $\tilde{z}_\ell = z_\ell - z^*_\ell$. The input to each spring ℓ is a relative velocity $w_\ell = (w_{x\ell}, w_{y\ell})$, while the output is the corresponding spring force $\tau_\ell = (\tau_{x\ell}, \tau_{y\ell})$.

For m springs let $z = (z_1, \ldots, z_m)$, $z^* = (z^*_1, \ldots, z^*_m)$, $\tilde{z} = (\tilde{z}_1, \ldots, \tilde{z}_m)$, $w = (w_1, \ldots, w_m)$, $\tau = (\tau_1, \ldots, \tau_m)$, and $K = \text{block.diag}\,(K_1, \ldots, K_m)$. We assume that the desired relative position z^* for the agents of the network is the prescribed vector $z^* \in (B^T \otimes I_2)x^*$, where B denotes the incidence matrix of the underlying tree graph which describes the interaction topology amongst the agents. The dynamics of the continuous virtual springs is well known [29,82] and given by

$$\begin{aligned} \dot{\tilde{z}} &= w, \\ \tau &= \frac{\partial H^c}{\partial \tilde{z}}, \end{aligned} \tag{7.9}$$

with Hamiltonian $H^c(\tilde{z}) = \frac{1}{2}\tilde{z}^T K \tilde{z}$. Note that the corresponding partial derivatives are given by

$$\frac{\partial H^c}{\partial \tilde{z}_{x\ell}} = k_{x\ell}\tilde{z}_{x\ell}, \quad \frac{\partial H^c}{\partial \tilde{z}_{y\ell}} = k_{y\ell}\tilde{z}_{x\ell}.$$

The coupling law to assign the virtual springs in between the agents [48] is given by

$$\begin{cases} u = -(B \otimes I_2)\tau, \\ w = (B^T \otimes I_2)y. \end{cases} \tag{7.10}$$

For the continuous springs, the closed-loop dynamics follows (7.6), (7.9), (7.10) and is given by

$$\begin{aligned} \dot{p} &= -(B \otimes I_2)\frac{\partial H}{\partial \tilde{z}} + u^r, \\ \dot{\tilde{z}} &= (B^T \otimes I_2)\frac{\partial H}{\partial p}. \end{aligned} \tag{7.11}$$

where $H(p, \tilde{z})$ is the closed-loop Hamiltonian given by

$$\begin{aligned} H(p, \tilde{z}) &= H^a(p) + H^c(\tilde{z}) \\ &= \frac{1}{2}p^T M^{-1} p + \frac{1}{2}\tilde{z}^T K \tilde{z}. \end{aligned} \tag{7.12}$$

Since all agents in the network are subject to Coulomb friction, the term u^r in (7.11) represents the friction and is equal to a set-valued map $u^r = -F(M^{-1}p)$, where $u_i^r = -F_i(M_i^{-1}p_i)$ from (7.3). Hence, the closed loop dynamics of the network is a differential inclusion given by

$$\begin{aligned} \dot{p} &\in -(B \otimes I_2)\frac{\partial H}{\partial \tilde{z}} - F(M^{-1}p), \\ \dot{\tilde{z}} &= (B^T \otimes I_2)\frac{\partial H}{\partial p}. \end{aligned} \tag{7.13}$$

Hence, the closed-loop dynamics can be written in a compact form $(\dot{p}, \dot{\tilde{z}}) \in \mathcal{K}_1(p, \tilde{z})$ with

$$\mathcal{K}_1(p, \tilde{z}) = \begin{pmatrix} -(B \otimes I_2)K\tilde{z} - F(M^{-1}p) \\ (B^T \otimes I_2)M^{-1}p \end{pmatrix},$$

where $F(M^{-1}p) = \times_{i=1}^{n} F_i(M_i^{-1}p_i)$. The map $F_i(M_i^{-1}p_i)$ follows (7.3) and it is given by

$$F_i(M_i^{-1}p_i) = \begin{cases} c_i \frac{M_i^{-1}p_i}{\|M_i^{-1}p_i\|} & \text{if } p_i \neq \mathbf{0} \\ B(\mathbf{0}, c_i) & \text{if } p_i = \mathbf{0}. \end{cases} \tag{7.14}$$

Note that $M_i^{-1}p_i$ ($M_i > 0$) is equal to the velocity of agent i. Before presenting the analysis of the closed-loop system controlled with continuous springs, we present some definitions on the terminal node and edge sets of the tree graph corresponding to the steps in the proof.

Definition 7.1 (Terminal node and edge set) *Let $\mathcal{V}^s$ denote the set of nodes for step s ($s \geq 1$), which is defined as $\mathcal{V}^s = \mathcal{V} - \bigcup_{r=0}^{s-1} \bar{\mathcal{V}}^r$. Here, $\bar{\mathcal{V}}^r$ denotes the set of terminal nodes, which is defined as*

$$\bar{\mathcal{V}}^r := \{ v_i \in \mathcal{V}^r | \deg v_i = 1 \},$$

with $\bar{\mathcal{V}}^0 = \emptyset$. In a similar way, let $\mathcal{E}^s$ denote the set of edges for step s, which is defined as $\mathcal{E}^s = \mathcal{E} - \bigcup_{r=0}^{s-1} \bar{\mathcal{E}}^r$. Here, $\bar{\mathcal{E}}^r$ denotes the set of terminal edges, which is defined as

$$\bar{\mathcal{E}}^r := \left\{ e_k \in \mathcal{E}^r | \, e_k = (v_i, v_j),\ v_i \in \bar{\mathcal{V}}^r \text{ or } v_j \in \bar{\mathcal{V}}^r \right\},$$

with $\bar{\mathcal{E}}^0 = \emptyset$.

We are now ready to present the result on the continuous springs.

Theorem 7.1 (Continuous virtual springs) *The solutions of the closed-loop dynamics* (7.13) *converge to the largest weakly invariant set where $p = \mathbf{0}$ and $\tilde{z}_\ell \in B(\mathbf{0}, \alpha_\ell)$ for all $\ell \in \mathcal{E}$, where α_ℓ is a positive constant depending on the spring constants $K_1, \ldots, K_m$ and Coulomb friction coefficients $c_1, \ldots, c_n$.*

Proof: Take the Hamiltonian $H(p, \tilde{z})$ in (7.12) as the Lyapunov function candidate. Since $H(p, \tilde{z})$ is continuously differentiable, the set-valued derivative $\dot{\tilde{H}}(p, \tilde{z})$ along (7.13) is

$$\dot{\tilde{H}}(p, \tilde{z}) = \{ \nabla H(p, \tilde{z}) \cdot w,\ w \in \mathcal{K}_1(p, \tilde{z}) \}.$$

By definition of $F(M^{-1}p)$ in (7.14), for any $w \in \mathcal{K}_1(p, \tilde{z})$ there exists $w^p \in F(M^{-1}p)$, $w^p = (w_1^p, \ldots, w_n^p)$, such that

$$w = \begin{pmatrix} -(B \otimes I_2)K\tilde{z} - w^p \\ (B^T \otimes I_2)M^{-1}p \end{pmatrix}.$$

Hence, $\dot{\tilde{H}}(p, \tilde{z}) = \{ a \in \mathbb{R} : a = -p^T M^{-T} w^p \} \subset (-\infty, 0]$. Therefore, applying the nonsmooth LaSalle's invariance principle [13], the solutions of the closed-loop system converge to the largest weakly invariant set of points $(p, \tilde{z})$ where $p = \mathbf{0}$ and

$$\left\{ (\mathbf{0}, \tilde{z}) \,\middle|\, \mathbf{0} = \begin{pmatrix} -w^p - (B \otimes I_2)K\tilde{z} \\ \mathbf{0} \end{pmatrix} \right\}. \tag{7.15}$$

Consider the tree graph $\mathcal{G}(\mathcal{V}, \mathcal{E})$ and define the terminal node-set $\bar{\mathcal{V}}^1$ and edge-set $\bar{\mathcal{E}}^1$ accordingly. From (7.15), for all $v_i \in \bar{\mathcal{V}}^1$ we have

$$\mathbf{0} = -w_i^p + \sum_{\ell \in \bar{\mathcal{E}}^1} b_{i\ell} K_\ell \tilde{z}_\ell,$$

where $w_i^p \in F_i(M_i^{-1} p_i)$. Note that, similar to z_ℓ, w_i^p belongs to $\mathbb{R}^2$ and it has a vector representation as $w_i^p = (w_{xi}^p, w_{yi}^p)$. Since v_i is a terminal node, the above equation simplifies to

$$\mathbf{0} = -w_i^p + b_{i\ell} K_\ell \tilde{z}_\ell, \tag{7.16}$$

since there is only one $b_{i\ell} \neq 0$ for each $v_i \in \bar{\mathcal{V}}^1$. From (7.16) it immediately follows that

$$\tilde{z}_\ell = b_{i\ell} K_\ell^{-1} \, w_i^p, \tag{7.17}$$

for all $k \in \bar{\mathcal{E}}^1$. Since $w_i^p \in B(\mathbf{0}, c_i)$, the equality (7.17) results in

$$\tilde{z}_\ell \in \left\{ e \middle| e = b_{i\ell} K_\ell^{-1} w_i^p, \; w_i^p \in B(\mathbf{0}, c_i) \right\},$$

and thus we can obtain a bound on the size (2-norm) of $\tilde{z}_\ell$ given by

$$\|\tilde{z}_\ell\| \in \left[0, c_i \, \sqrt{\operatorname{tr}\left(K_\ell^{-1} \, (K_\ell^{-1})^T \right)} \right].$$

Recall that $K_\ell = \operatorname{diag} k_{x\ell}, k_{y\ell}$. Then, the above equation implies

$$\|\tilde{z}_\ell\| \in \left[0, \frac{c_i}{k_{x\ell} k_{y\ell}} \, \sqrt{k_{x\ell}^2 + k_{y\ell}^2} \right].$$

In this way we find a bound for all springs corresponding to an edge in the terminal edge set $\bar{\mathcal{E}}^1$.

Now consider the node set $\mathcal{V}^2$ and edge set $\mathcal{E}^2$ (see Definition 7.1) and the corresponding terminal sets $\bar{\mathcal{V}}^2$ and $\bar{\mathcal{E}}^2$. Similar to the previous step, for all $v_i \in \bar{\mathcal{V}}^2$, we have

$$\mathbf{0} = -w_i^p + \sum_{\ell \in \mathcal{E}} b_{i\ell} K_\ell \tilde{z}_\ell. \tag{7.18}$$

We rewrite (7.18) as

$$\mathbf{0} = -w_i^p + \sum_{k \in \bar{\mathcal{E}}^1} b_{ik} K_k \tilde{z}_k + \sum_{\ell \in \bar{\mathcal{E}}^2} b_{i\ell} K_\ell \tilde{z}_\ell. \tag{7.19}$$

Similar to the first step, there is exactly one $b_{i\ell} \neq 0$ for all $v_i \in \bar{\mathcal{V}}^2, e_\ell \in \bar{\mathcal{E}}^2$. In addition, each $\tilde{z}_k \in \bar{\mathcal{E}}^1$ follows (7.17). Therefore, we obtain

$$b_{i\ell} K_\ell \tilde{z}_\ell \in \left\{ e \middle| e = w_i^p - \sum_{j \in \bar{\mathcal{V}}^1} w_j^p, \quad w_j^p \in B(\mathbf{0}, c_j), \, w_i^p \in B(\mathbf{0}, c_i) \right\}.$$

Hence, we find a bound for all springs corresponding to an edge in the terminal edge set $\bar{\mathcal{E}}^2$. Repeating the steps above until $\bigcup_i \bar{\mathcal{E}}^i = \mathcal{E}$, we find a bound for all springs in the graph, depending on the friction coefficients $c_1, \ldots, c_n$ and spring constants $K_1, \ldots, K_m$, which completes the proof. □

7.2.3 Discontinuous (binary) virtual springs

The previous section showed that continuous virtual springs can not achieve the formation objectives (7.1) exactly. Motivated by the example in Section 7.1 we replace the continuous virtual springs by its discontinuous counterpart. Using the same variables as in (7.9), the dynamics of m discontinuous springs is given by

$$\begin{aligned} \dot{\tilde{z}} &= w \\ \tau &= \partial H^d \end{aligned} \tag{7.20}$$

with a locally Lipschitz Hamiltonian $H^d(\tilde{z}) = \|K\tilde{z}\|_1$, where $\|K\tilde{z}\|_1$ denotes the one-norm that is $\|K\tilde{z}\|_1 = \sum_{\ell=1}^{m} (k_{x\ell}|\tilde{z}_{x\ell}| + k_{y\ell}|\tilde{z}_{y\ell}|)$. Since H^d is a nonsmooth Hamiltonian function([32]), it is not differentiable everywhere. Hence, we calculate ∂H^d based on the Clarke generalized gradient (see Chapter 2, Definition 2.6).

Using the same coupling law (7.10) for the continuous springs, the closed-loop dynamics for the discontinuous springs follows directly from (7.6), (7.10), (7.20) and is given by

$$\begin{aligned} \dot{p} &\in -(B \otimes I_2)\partial_{\tilde{z}} H - F(M^{-1}p) \\ \dot{\tilde{z}} &= (B^T \otimes I_2)\frac{\partial H}{\partial p}, \end{aligned} \tag{7.21}$$

where $\partial_{\tilde{z}} H(\tilde{z}) = \partial H^d(\tilde{z})$ and $H(p, \tilde{z})$ is the closed-loop Hamiltonian given by

$$\begin{aligned} H(p, \tilde{z}) &= H^a(p) + H^d(\tilde{z}) \\ &= \frac{1}{2} p^T M^{-1} p + \|K\tilde{z}\|_1. \end{aligned} \tag{7.22}$$

Note that (7.21) is a differential inclusion due to the set-valued model of Coulomb friction and the discontinuous spring force ∂H^d. Here, $\partial H^d = K\,\mathcal{K}\text{sign}\tilde{z}$ where $\mathcal{K}\text{sign}\tilde{z} = \times_{\ell=1}^{m} \mathcal{K}\text{sign}\tilde{z}_\ell$ with

$$\mathcal{K}\text{sign}\tilde{z}_\ell = \begin{cases} \{\frac{\tilde{z}_{x\ell}}{|\tilde{z}_{x\ell}|}\} \times \{\frac{\tilde{z}_{y\ell}}{|\tilde{z}_{y\ell}|}\} & \text{if } \tilde{z}_{x\ell} \neq 0, \tilde{z}_{y\ell} \neq 0 \\ [-1, +1] \times \{\frac{\tilde{z}_{y\ell}}{|\tilde{z}_{y\ell}|}\} & \text{if } \tilde{z}_{x\ell} = 0, \tilde{z}_{y\ell} \neq 0 \\ \{\frac{\tilde{z}_{x\ell}}{|\tilde{z}_{x\ell}|}\} \times [-1, +1] & \text{if } \tilde{z}_{x\ell} \neq 0, \tilde{z}_{y\ell} = 0 \\ [-1, +1] \times [-1, +1] & \text{if } \tilde{z}_{x\ell} = 0, \tilde{z}_{y\ell} = 0. \end{cases} \tag{7.23}$$

Note that (7.23) considers discontinuous springs along x and y separately. This is a design choice that complies with the position-based control design as stated in Section 7.2.2. Now, let write the closed-loop dynamics in a compact form $(\dot{p}, \dot{\tilde{z}}) \in \mathcal{K}_2(p, \tilde{z})$

$$\mathcal{K}_2(p, \tilde{z}) = \begin{pmatrix} -(B \otimes I_2)K\ \mathcal{K}\text{sign}\tilde{z} - F(M^{-1}p) \\ (B^T \otimes I_2)M^{-1}p \end{pmatrix}, \tag{7.24}$$

where $F(M^{-1}p)$ is defined in (7.14). Now we are ready to formulate our main result:

Theorem 7.2 (Discontinuous springs) *Assume that* $\min\{k_{x\ell}, k_{y\ell}\} > \max\{c_i, c_j\}$ *for* $e_\ell = (n_i, n_j) \in \mathcal{E}$. *Then the solutions of the closed-loop dynamics* (7.21) *converge to the origin* $(p, \tilde{z}) = (\mathbf{0}, \mathbf{0})$, *thereby achieving the control objectives* (7.1).

Proof: Take the Hamiltonian in (7.22) as the candidate Lyapunov function which is a regular and locally Lipschitz function. Since the Hamiltonian is not differentiable everywhere, first we calculate its corresponding Clarke generalized gradients $\partial H(p, \tilde{z})$ [3] as

$$\partial H(p, \tilde{z}) = \left\{ v \,:\, v = \begin{pmatrix} M^{-1}p \\ Kv^{\tilde{z}} \end{pmatrix} \text{ s.t. } v_k^{\tilde{z}} \in \mathcal{K}\,\text{sign}\tilde{z}_k \right\}. \tag{7.25}$$

Calculating the set-valued derivative $\dot{\tilde{H}}(p,\tilde{z})$ along (7.21), we obtain

$$\dot{\tilde{H}}(p,\tilde{z}) = \big\{a \in \mathbb{R} \,:\, \exists w \in \mathcal{K}_2(p,\tilde{z}) \text{ s.t. } a = w \cdot v, \text{ for all } v \in \partial H(p,\tilde{z})\big\}.$$

By definition of $\mathcal{K}_2(p,\tilde{z})$ in (7.23)-(7.24), for any $w \in \mathcal{K}_2(p,\tilde{z})$ there exists $w^p \in F(M^{-1}p)$ and $w^{\tilde{z}} \in \mathcal{K}\text{sign}\tilde{z}$ such that

$$w = \begin{pmatrix} -(B \otimes I_2)Kw^{\tilde{z}} - w^p \\ (B^T \otimes I_2)M^{-1}p \end{pmatrix}.$$

For each $v \in \partial H(p,\tilde{z})$, choose $w^{\tilde{z}} = v^{\tilde{z}}$. Hence, we obtain $\dot{\tilde{H}}(p,\tilde{z}) = \{a \in \mathbb{R} : a = -p^T M^{-T} w^p\} \subset (-\infty, 0]$. Assume that $\dot{\tilde{H}} \neq \emptyset$. Therefore, applying the nonsmooth version of LaSalle's invariance principle, the solutions of the closed-loop system converge to the largest weakly invariant set of points $(p,\tilde{z})$ such that $p = \mathbf{0}$ and

$$\left\{(\mathbf{0},\tilde{z}) \,\middle|\, \mathbf{0} = \begin{pmatrix} -w^p - (B \otimes I_2)\, K w^{\tilde{z}} \\ \mathbf{0} \end{pmatrix}\right\}, \tag{7.26}$$

where $w^p \in \mathbb{R}^2$ and $w^{\tilde{z}} \in \mathbb{R}^2$. Now, consider the tree graph $\mathcal{G}(\mathcal{V},\mathcal{E})$ and define the terminal node-set $\bar{\mathcal{V}}^1$ and edge-set $\bar{\mathcal{E}}^1$ accordingly. Based on (7.26), all nodes $v_i \in \bar{\mathcal{V}}^1$ obey

$$\mathbf{0} = w_i^p + \sum_{\ell \in \bar{\mathcal{E}}} b_{i\ell} K_\ell w^{\tilde{z}_\ell}.$$

Noting that v_i is a terminal node, the above equation simplifies to

$$\mathbf{0} = w_i^p + b_{i\ell} K_\ell w^{\tilde{z}_\ell}, \tag{7.27}$$

where $w_i^p = (w_{xi}^p, w_{yi}^p)$, $w_i^p \in B(\mathbf{0}, c_i)$ and $w^{\tilde{z}_\ell} = (w_x^{\tilde{z}_\ell}, w_y^{\tilde{z}_\ell})$. Writing (7.27) for each of the components of w_i^p, we obtain

$$0 = w_{xi}^p + b_{i\ell} k_{x\ell} w_x^{\tilde{z}_\ell} \tag{7.28}$$

$$0 = w_{yi}^p + b_{i\ell} k_{y\ell} w_y^{\tilde{z}_\ell}. \tag{7.29}$$

We will now prove Theorem 7.2 by contradiction. Consider (7.28) and assume that $\tilde{z}_{x\ell} \neq 0$, then $w_x^{\tilde{z}_\ell}$ is equal to either $+1$ or -1. Moreover, since $w_i^p \in B(\mathbf{0}, c_i)$, we have $w_{xi}^p \in [-c_i, c_i]$. Take $w_x^{\tilde{z}_\ell} = +1$, then from (7.28) we obtain

$$w_{xi}^p + b_{i\ell} k_{x\ell} w_x^{\tilde{z}_\ell} \in [-c_i + k_{x\ell}, c_i + k_{x\ell}]$$

By assumption, we have $k_{x\ell} > c_i$. Hence, both of the upper and lower bounds of the above interval are positive and zero cannot belong to this interval. Similarly, if $w_x^{\tilde{z}_\ell} = -1$, we obtain the interval $[-c_i - k_{x\ell}, c_i - k_{x\ell}]$ where both of its bounds are negative. This result contradicts (7.28). As a result, $\tilde{z}_{x\ell}$ should necessarily be zero. A similar argument holds for y-direction (7.29) which results in $\tilde{z}_{y\ell} = 0$. In this way we show that for all springs corresponding to an edge in the terminal edge set $\bar{\mathcal{E}}^1$, the error position $\tilde{z}_\ell$ is equal

to zero on the invariant set (7.26).
Now consider the node set $\mathcal{V}^2$ and edge set $\mathcal{E}^2$ and the corresponding terminal sets $\bar{\mathcal{V}}^2$ and $\bar{\mathcal{E}}^2$. Using similar arguments as above, we can show that the relative error position is equal to zero for all springs corresponding to an edge in the terminal edge set $\bar{\mathcal{E}}^2$.
Repeating the steps above until $\bigcup_i \bar{\mathcal{E}}^i = \mathcal{E}$, we can conclude that for each of edges in the graph the corresponding relative position error converges zero, thereby completing the proof. □

7.3 Simulations

In this section, we present simulation results illustrating Theorems 7.1 and 7.2. Consider a network of $n = 5$ agents interconnected using $m = 4$ virtual couplings. The associated incidence matrix is equal to $B = (B_1^T \dots B_5^T)^T$ with $B_1 = (-1\ 0\ 0\ 0\ 0)$, $B_2 = (+1\ -1\ -1\ 0\ 0\ 0)$, $B_3 = (0\ +1\ 0\ -1\ -1\ 0)$, $B_4 = (0\ 0\ +1\ +1\ 0\ -1)$, $B_5 = (0\ 0\ 0\ 0\ +1\ +1)$. Each agent has the unit mass ($m_i = 1$). The Coulomb friction coefficient is set equal to $c_i = 2$ for $i = 1, \dots, 5$. For the virtual couplings we set $k_{x\ell} = k_{y\ell} = 2.5$ for $\ell = 1, \dots, 4$ (i.e., the condition $\min\{k_{x\ell}, k_{y\ell}\} > \max\{c_i, c_j\}$ in Theorem 7.2 is satisfied).

The desired formation has a pentagon shape with edge length equal to two and is defined by the following inter-agent position vectors: $z_1^* = (0, -2)$, $z_2^* = (-1, -1 - \sqrt{3})$, $z_3^* = (-1, 1 + \sqrt{3})$, $z_4^* = (0, 2)$. The initial conditions for the agents are set as $q_{xi}(0) = (0.5, 0.2, -1, 2, 0.8)$ and $q_{yi}(0) = (1, -0.2, 0.9, 1.5, 0)$. The simulations are done using MATLAB with a fixed-step solver (ode4, step size=0.001). Fig. 7.3 and Fig. 7.4 show the time evolution of the error relative position $\tilde{z}_x = z_x - z_x^*$, momentum p_x, and control input u_x along the x direction for the continuous springs (Theorem 7.1) and the discontinuous springs (Theorem 7.2) respectively. The time evolution of the relative position $\tilde{z}_y$, momentum p_y and control input u_y along the y direction follow similar trends.

The top plot in Fig. 7.3 shows that the relative position z does not converge to the desired one, z^*, using continuous springs. However, using discontinuous springs the relative position z does converge to the desired prescribed relative position z^* (see Fig. 7.4, top). The middle plots in Fig. 7.3 and Fig. 7.4 show that p_x converges to zero for both types of springs.

Comparing the control action u_x in (Fig. 7.3, bottom) and (Fig. 7.4, bottom), the control action related to the discontinuous spring shows a fast switching behavior while $\tilde{z}_x$ converges to zero.

In Chapter 3, some potential solutions have been proposed to deal with the fast oscillations. As an example and motivated by hysteretic quantizers in [11], here, we include the simulation result of the time evolution of the system using a hysteretic-quantizer based sign function (see Chapter 3). Fig. 7.5 shows the time evolution of $\tilde{z}_x$, p_x and u_x with a hysteretic sign controller. The model and the analysis of such a controller are beyond the scope of this chapter. For the sake of clarity, only the control action of one of the agents is shown. As shown, the oscillations of the control action in Fig. 7.5 is highly

reduced compared with Fig. 7.4.

7.4 Conclusions

This chapter has analyzed the problem of formation control of a group of agents communicating over a tree graph in the presence of Coulomb friction. Two types of controllers (virtual springs) have been presented to achieve the formation objective. Using tools from nonsmooth analysis, it has been shown that the continuous virtual springs can not achieve exact formations. Binary virtual springs on the other hand can achieve a desired formation exactly, under the condition that the virtual spring constant is strictly larger than the Coulomb friction coefficient. Directions for future research include generalization of the types of graphs and mitigating the undesired fast switching of the control action related to the discontinuous springs e.g. by the methods presented in Chapter 3.

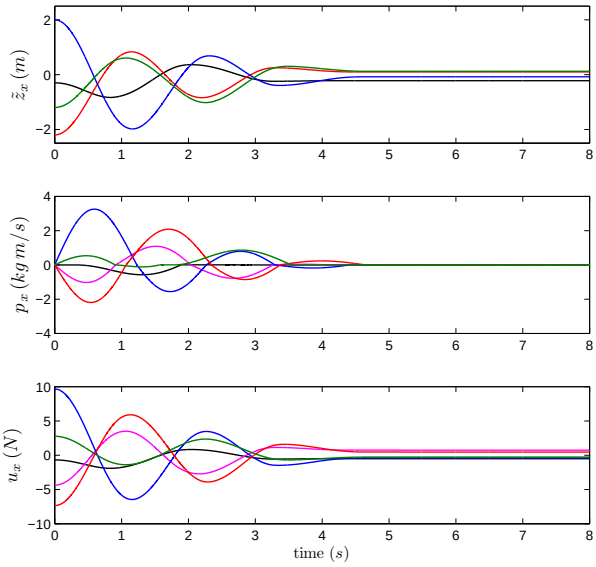

Figure 7.3: Time evolution of the relative position $\tilde{z}_x$, momentum p_x, and control input u_x using continuous springs.

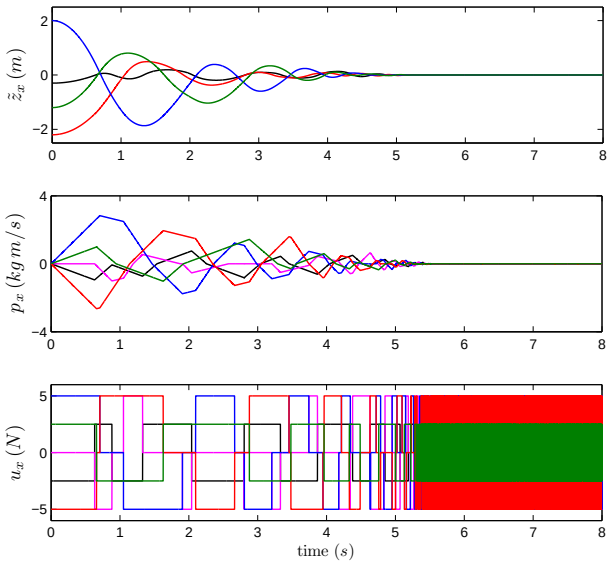

Figure 7.4: Time evolution of the relative position $\tilde{z}_x$, momentum p_x, and control input u_x using discontinuous springs.

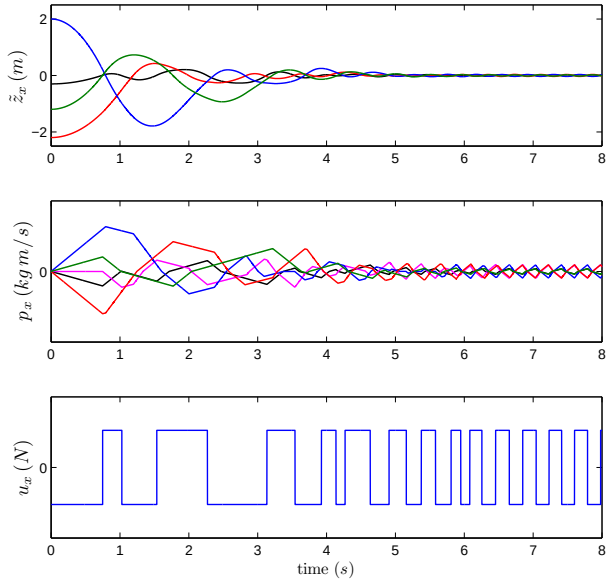

Figure 7.5: Time evolution of the relative position $\tilde{z}_x$ and momentum p_x of all agents together with the control input u_x of agent 1 using hysteretic discontinuous springs.